Available online at www.sciencedirect.com

ScienceDirect

ARTICLE

Influence of Annealing Time on Σ3 Boundary and Σ9 Boundary Evolutions in Hastelloy C-276 Alloy

Zhang Xiaoyu[1,2],   Li Defu[1],   Guo Shengli[1],   Zhao Xianming[2]

[1] *Beijing General Research Institute for Nonferrous Metals, Beijing 100088, China;* [2] *State Key Laboratory of Rolling and Automation, Northeastern University, Shenyang 110004, China*

Abstract: Hastelloy C-276 was subjected to low strain deformation and then annealed at 1100 °C for different time. The Σ3 and Σ9 boundary percentages and grain boundary plane distributions were characterized by electron back-scatter diffraction (EBSD) and a five-parameter analysis method. The results show that the Σ3 boundary evolves towards a more exact coincident-site lattice (CSL) misorientation and the Σ3 boundary plane is closer to low surface energy plane {111} with the increasing of annealing time. This is consistent with *fine tuning* mechanism. While the population of incoherent Σ3 boundary is increasing, the proportion of Σ9 boundary with larger deviations increase, too. And the distributions of grain boundary density planes for Σ9 boundary are more intensive on the whole [110] zone.

Key words: Hastelloy C-276; Σ3 and Σ9 boundary; grain boundary plane distribution; EBSD

Hastelloy C-276 alloy is a Ni-Cr-Mo alloy that is generally regarded as a versatile corrosion-resistant alloy. Due to its good high temperature strength, high resistance to neutron radiation and corrosive environment abilities, it has been widely used in chemical, oil and nuclear industries[1,2]. In particular, Hastelloy C-276 is being selected as a potential candidate material in construction of different components of Gen IV reactors [3]. However, to be suitable for the Gen IV designed environment, some modifications of material's structure should be considered. The present reports[4,5] state that grain boundary characteristics strongly affect the properties of material.

Grain boundary engineering (GBE) is a method of manipulating the grain boundaries in a microstructure so that a higher fraction of 'special' boundaries is obtained. The 'special' boundaries are essentially low sigma coincident-site lattice (CSL) boundaries. These boundaries are different from random high angle boundaries in properties of grain boundary energy and migration. The 'special' boundaries are brought about by suitable thermos-mechanical processing in body centred cubic materials. Grain boundary engineering can improve material properties like ductility, corrosion and oxidation resistance, creep and fracture resistance[5,6].

Grain boundary properties depend on both the lattice misorientation and the orientation of the grain boundary plane[7]. Grain boundaries with low-index surfaces have relatively low energies. The observations suggest[8] that a 'special' grain boundary should be defined as one that is terminated by at least one low-index plane. Saylor et al. [9] have developed a stereological procedure to determine the distribution of boundary planes from orientation maps on single planar sections. This technique, known as five-parameter analysis, coupled with automated trace analysis software was used to extract the five-parameter distribution from EBSD maps. The five-parameter area distributions are expressed as 'multiples of a random distribution' (MRD).

The aim of the present report was to investigate the evolutions of Σ3 and Σ9 boundaries with annealing time. We employ the five-parameter stereology to reveal the distributions of Σ3 and Σ9 grain boundary plane orientations in Hastelloy C-276 annealed for different time. The data will be interpreted with the distribution of boundary planes and its

consequences for our understanding of the Σ3 and Σ9 boundary evolutions.

1 Experiment

1 mm thick Hastelloy C-276 sheet whose chemical composition (wt%) was 15.07 Cr, 15.53 Mo, 4.14 Fe, 4.04 W, 2.5 Co, 0.62 Mn, 0.01 P, 0.08 Si, 0.012 C, 0.002 S and Bal. Ni, was solution-heat treated at 1150 ℃ for 0.5 h and then used for processing. The samples were cold rolled with thickness reduction of 5%. The cold-worked samples were afterwards annealed at 1100 ℃ for 0.25~1 h.

The surfaces of samples were firstly ground with SiC and diamond abrasives, then they were electropolished in an electrolyte containing $H_2SO_4:CH_3COOH=1:4$ at room temperature. The fractions of special boundaries were determined by electron backscatter diffraction (EBSD) using a JEOL JSM7001LV SEM with EDAX (TSL) OIM Data Collection 6.0 software. The OIM analysis software was then used to extract the boundary line traces from the samples. The five-parameter grain boundary distribution (FPGBD) was determined from these traces using a procedure described previously[9]. Part of the procedure was segmentation of curved grain boundaries. The Brandon Criterion[10] was used to classify CSL boundaries, as a fraction of total boundary length. The proportion of misorientations on specific axes ([110], [111]) was calculated with a tolerance of ±5°. The resolution of the distribution is approximately 10° and all distributions are plotted in stereographic projection.

2 Results

2.1 Fractions of Σ3 boundary and Σ9 boundary

As shown in Fig.1 we can see that the fraction of Σ3 boundary increases from 58.7% to 60.2% as the time is prolonged to 15 min. After that, the fraction falls to 57%. There is a peak percentage at 15 min. The trend illustrates that any longer annealing time cannot affect the increase of Σ3 boundary, the rational processing should be adapted with right time. The conclusions are consistent with the results of S. L. Lee researches [11]. The Σ9 boundary percentage is less than 3%. There are small changes with increasing annealing time. However, the tendency of Σ9 boundary does not correspond to the tendency of Σ3 boundary, because the peak percentage of the Σ9 boundary is at 30 min. This may be due to the reaction of the boundaries: Σ3+Σ3→Σ9.

The EBSD map of the 5% thickness reduction annealed at 1100 ℃ for different time is shown in Fig.2. The Σ3 boundaries are colored red lines. They indicate that the main boundaries are

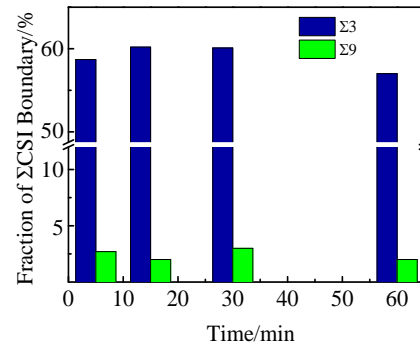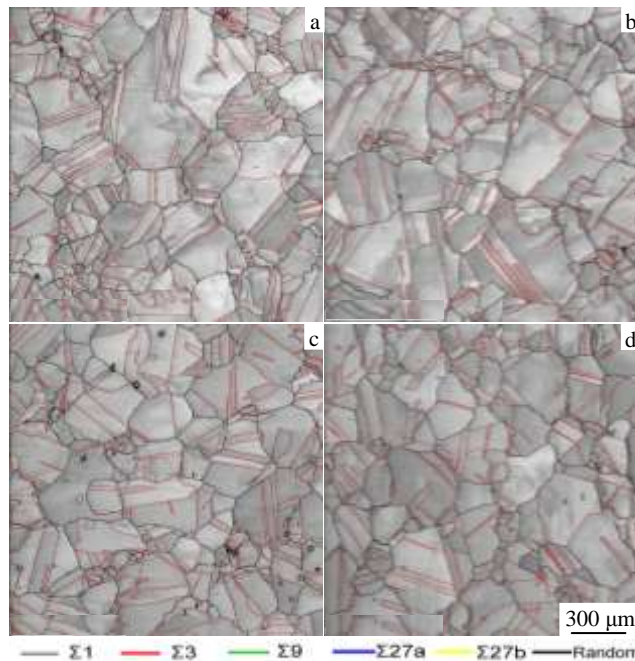Fig.1　Fractions of Σ3 boundary and Σ9 boundary of Hastelloy C-276 annealed at 1100 ℃ for different time

Fig.2　Grain boundary images of quality (IQ) map of 5% strain annealed at 1100 ℃ for various time: (a) 5 min, (b) 15 min, (c) 30 min, and (d) 60 min

Σ3 boundaries, and most of them are in the shape of a straight single line or parallel line pairs within grains. And few island and curved incoherent Σ3 boundaries are obtained in these maps. The microstructure consists of equiaxed grains ranging between 30 μm and 260 μm in size as shown in Fig.2a. With extended time, the average grain size has a small decrease from 101 μm to 89 μm (Fig.2d).

2.2 Evolutions of Σ3 boundary and Σ9 boundary plane during annealing

In all of the projections, the [001] crystal axis is perpendicular to the plane of the paper and the [100] direction is horizontal in the plane of the paper, pointing to the right. The distributions of Σ3 boundary plane are plotted in standard stereographic projection in Fig.3. The relative areas of Σ3 boundary planes are centred on {111} planes. And they show a preference for <111> misorientation axes twist boundaries. The MRD values are not increased with the increasing of annealing time in Fig.3. On the contrary, the maximum proportion of Σ3 boundary is in the sample annealed at 15 min and the MRD valves are not the peak. It illustrates that many Σ3 boundaries cannot terminate on {111} plane, and there are a lot of incoherent Σ3 boundaries in the sample annealed for 15 min.

The distributions of grain boundary density planes for Σ9 (39 °/[110]) section annealed at 1100 ℃ for various time are shown in Fig. 4. In the section for Σ9 there are multiple peaks on the [110] zone. The predominant maxima along the [110] zone indicate that most of the segments have a tilt character. Note that the maximum along the tilt zone is found at the tilt boundary (114) in Fig.4a. However, the maximum MRD values

on the [110] zone are at the symmetric (221) and ($\overline{1}\overline{1}$2) in Fig.4b. For extended time, the maximum along the tilt zone is more intensive on the whole [110] zone. The maxima appear to be confined more narrowly on the [110] zone.

The change in proximity factor for the Σ3 boundary with the increasing of annealing time can be rationalized as an overall reduction of accumulated strains in the microstructure, which are associated with local lattice rotations. The Σ3 boundary deviations are small with the increasing of annealing time, and this is reported [12] by Thomson in the annealing process of strain-annealed nickel. And the Σ9 boundary deviations are very larger for annealing periods of 15 and 30 min. This is closely related to the interactions of Σ3ⁿ boundaries.

3 Discussions

In Fig.1, the peak of Σ3 boundary percentage is in the sample annealed at 15 min, whereas the MRD values of {111} planes decrease in Fig.3b. The decrease of MRD values in {111} planes indicates most of the additional Σ3 population is incoherent twins, because coherent annealing twins would have been on {111}. According to the paper results[13], a coherent twin and one vicinal-to-{111} Σ3 (incoherent twin) boundary meet at a triple junction generated Σ9 boundaries with high deviations. While the population of incoherent Σ3 boundary is increasing, the larger deviations Σ9 boundary proportion also increases. It can be seen from Fig.5 and Fig.6, the MRD values of Σ9 boundary planes are lower and the deviations of Σ9 boundaries are larger for annealing periods of 15 and 30 min.
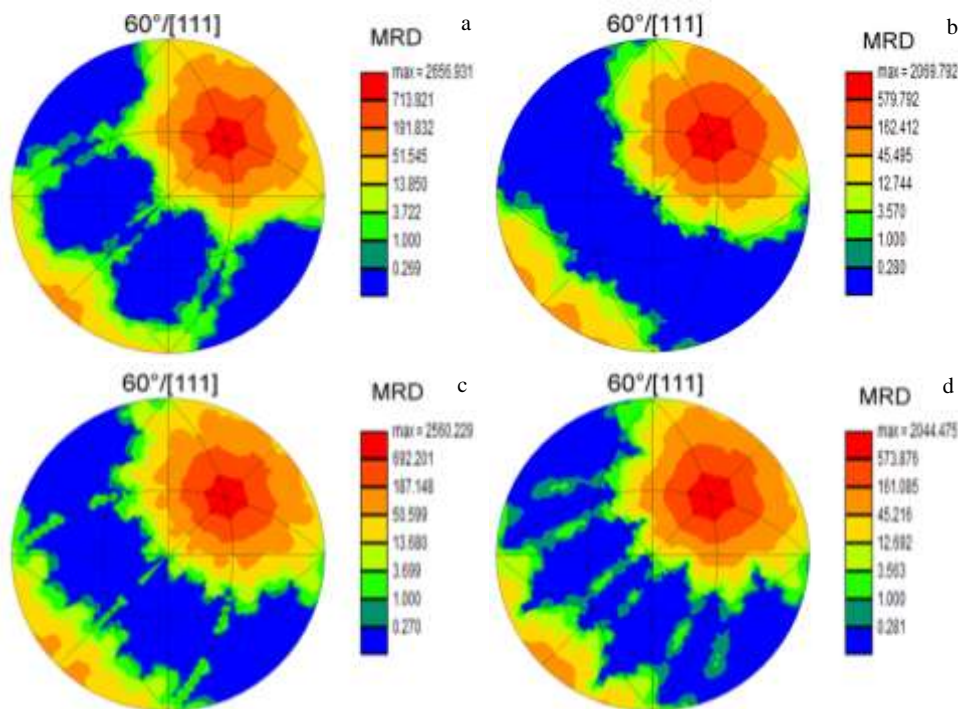

Fig.3 Distributions of grain boundary density planes for Σ3 (60 °/[111]) section annealed at 1100 ℃ for various time: (a) 5 min, (b) 15 min, (c) 30 min, and (d) 60 min
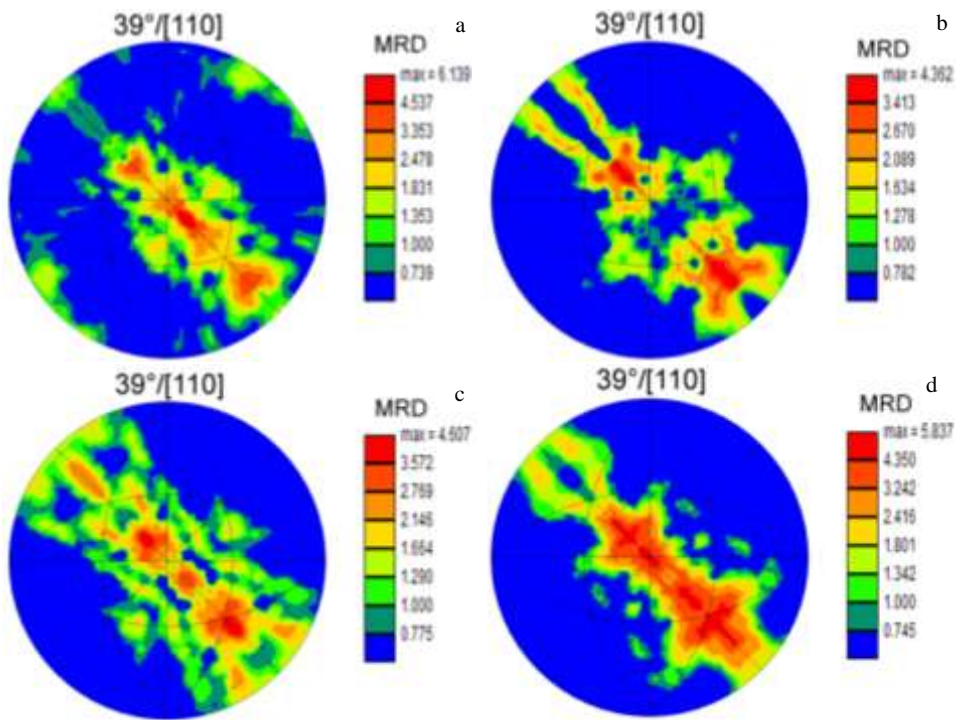
Fig.4   Distributions of grain boundary density planes for Σ9(39°/[110]) section annealed at 1100 °C for various time: (a) 5 min, (b) 15 min, (c) 30 min, and (d) 60 min

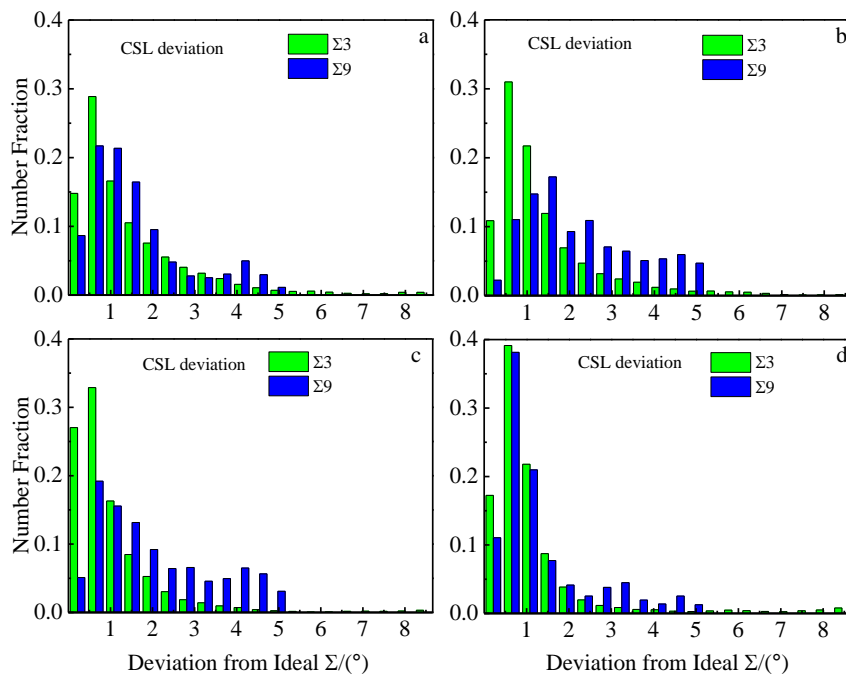

Fig.5   Number fraction of Σ3 boundary and Σ9 boundary deviations from ideal ΣCSL boundaries at different annealing time: (a) 5 min, (b) 15 min, (c) 30 min, and (d) 60 min

The most common plane presented in nickel-based materials is the plane with the lowest surface energy, {111}. This tendency for boundaries to terminate on low surface energy planes has been observed in face-centred cubic materials, and the dominance of {111} boundary planes has been recorded in nickel specimens[14]. Hence, the Σ3 boundary evolves towards a more exact CSL misorientation during annealing. The present data further confirm this preponderance of low surface energy planes as a general trend, as shown in Fig.6. That explains the proportion of coherent Σ3 boundaries
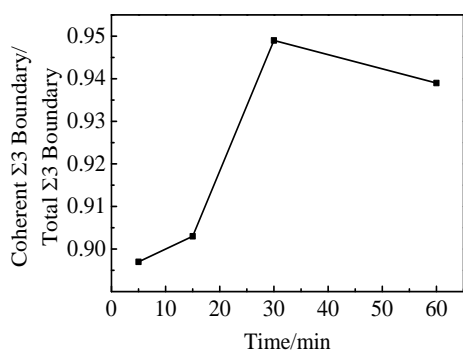
Fig.6　Change of ratio (coherent Σ3 boundary/total Σ3 boundary) with annealing time

(the deviations from the reference misorientation are ≤3°) are larger with the increasing of annealing time. This is in agreement with the *fine tuning* mechanisms [15], i.e. the Σ3 boundary evolves to closer CSL matching, and the deviation is reduced by local lattice rotation near the boundary, probably accompanied by boundary plane reorientation.

The aim of GBE is to get more 'special' grain boundaries with low surface energy planes. Prolonging annealing time is useful during the GBE processing. Applying the GBE technique to manufacture products for enhancing the grain boundary related properties is the final goal of the GBE researches.

4　Conclusions

1) Reasonable annealing time can promote the frequency of Σ3 boundary increasing, and Σ3 boundary evolves towards a more exact CSL misorientation with the increasing of annealing time. This is in agreement with the *fine tuning* mechanisms.

2) The proportion of Σ9 boundary with high deviations is larger due to the increasing of incoherent Σ3 boundary population, according to the interaction: Σ3+Σ3→Σ9.

References

1　Akhter J I, Shaikh M A, Ahmad M *et al. Journal of Materials Science Letters*[J], 2001, 20(4): 333
2　Hashim M, Babu K E S R, Duraiselvam M *et al. Materials & Design*[J], 2013, 46: 546
3　Zhang Q, Tang R, Yin K *et al. Corrosion Science*[J], 2009, 51(9): 2092
4　Watanabe T, Tsurekawa S, Kobayashi S *et al. Materials Science and Engineering A*[J], 2005, 410: 140
5　Randle V. *Acta Materialia*[J], 2004, 52(14): 4067
6　Kobayashi S, Hirata M, Tsurekawa S *et al. Procedia Engineering*[J], 2011, 10: 112
7　Rohrer G S, Randle V, Kim C S *et al. Acta Materialia*[J], 2006, 54(17): 4489
8　Randle V. *Scripta Materialia*[J], 2006, 54(6): 1011
9　Saylor D M, El-Dasher B S, Adams B L *et al. Metallurgical and Materials Transactions A*[J], 2004, 35(7): 1981
10　Brandon D G. *Acta Metall*[J], 1966,14: 1479
11　Lee S L, Richards N L. *Materials Science and Engineering A*[J], 2005, 405(1): 74
12　Thomson C B, Randle V. *Textures and Microstructures*[J], 1996, 28(1): 71
13　Randle V, Hu Y. *Journal of Materials Science*[J], 2005, 40(12): 3243
14　Randle V, Rohrer G S, Miller H M *et al. Acta Materialia*[J], 2008, 56(10): 2363
15　Thomson C B, Randle V. *Acta Materialia*[J], 1997, 45(12): 4909

Hastelloy C-276 合金 Σ3 晶界和 Σ9 晶界随着退火时间的演变规律

张晓宇 [1,2]，李德富 [1]，郭胜利 [1]，赵宪明 [2]

(1. 北京有色金属研究总院，北京 100088)

(2. 东北大学 轧制技术及连轧自动化国家重点实验室，辽宁 沈阳 110004)

摘　要：Hastelloy C-276 合金经小变形量冷轧后进行 1100 ℃不同时间的退火处理。采用 EBSD 技术对 Σ3 和 Σ9 晶界比例进行统计，同时采用五参数法对 Σ3 和 Σ9 晶界面分布进行分析。结果表明，Σ3 晶界随着退火时间的延长更加接近于标准重合点阵晶界取向，而其晶界面更加接近于低能量的{111}晶界面。这一结果符合晶界"微调"机制。Σ9 晶界面分布则越来越集中在[110]晶带。而偏差较大的 Σ9 晶界比例增加，是由于非共格 Σ3 比例的增加导致的。

关键词：Hastelloy C-276 合金；Σ3 和 Σ9 晶界；晶界面分布；EBSD

作者简介：张晓宇，男，1985 年生，博士，北京有色金属研究总院加工事业部，北京 100088，电话：010-61771755，E-mail: xy12152006@126.com